DOI: 10.1002/srin.201000026 steel research int. 81 (2010) No. 6

Modelling of Heat Transfer, Dendrite Microstructure and Grain Size in Continuous Casting of Steels

V. Karlinski de Barcellos[1)*], V. Lopes da Silva Gschwenter[1)], H. Kytönen[3)], C. Alexandre dos Santos[2)], J. Alvares Spim[1)], S. Louhenkilpi[3)], and J. Miettinen[3)]

[1)] Federal University of Rio Grande do Sul (UFRGS), Foundry Laboratory (LAFUN) – Center of Technology (CT), P.O. Box 15.021, 91501-970, Porto Alegre/RS – Brazil, vinicius.karlinski@ufrgs.br
[2)] Pontifical Catholic University of Rio Grande do Sul (PUCRS), Nucleus of Metallic Materials Engineering (NUCLEMAT), 90.619-900 - Porto Alegre/RS – Brazil
[3)] Helsinki University of Technology (TKK), Laboratory of Metallurgy, P.O. Box 6200, FI-02150 Espoo – Finland
* Corresponding author

The dendrite arm spacing and grain size in continuous casting has been studied by mathematical modelling and experimental measurements. Two in-house tools have been used in the study. The heat transfer is calculated by the model called TEMPSIMU and the solidification as well as the microstructural phenomena by the thermodynamic-kinetic software called IDS. The models are validated by comparison the calculated results with experiments from steel plants. In continuous casting, the solidification structure is also influenced by process parameters. In this study the effect casting speed, superheat and secondary cooling on arm spacings and grain size is also studied. The in-house models and the obtained results are presented in this paper. Using the developed models, the heat transfer and microstructure can be controlled more accurately.

Keywords: solidification, heat transfer, dendrite arm spacing, grain size

Submitted on 14 December 2009, accepted on 23 February 2010

Introduction

Continuous casting involves many physical phenomena. The main phenomena are: fluid flow, heat transfer and solidification. In recent years, a lot of different kinds of heat transfer and microstructural models for continuous casting have been presented. Most of the heat transfer models developed do not calculate the fluid flow. In these models, it is assumed that the strand (solid and liquid) is withdrawn through the machine with a constant velocity field (= casting speed). The convective heat transfer generated by the fluid flow is taken into account by using an effective thermal heat conductivity method. This simplification does not affect very much the results in the solidifying shell. For this purpose, numerical models used for heat transfer simulations are nowadays relative accurate taking into account the most important phenomena. However, to obtain realistic results, accurate data on the thermophysical material properties and boundary conditions are also needed.

In the past twenty years, modelling of microstructure has reached a relatively mature state with two different modelling philosophies: (1) the models are (semi)empirical (black box) or (2) physically-based (fundamental) models (white box). Both concepts have their merits. Empirical models are fast but they can be applied only to specific cases they are made for. Fundamental models are more general and they could be applied to more complex applications. However, in general, fundamental models are not yet developed as far as they could be used alone for complex industrial cases. The fundamental models also need much more calculation time than the empirical models.

The most popular physically-based modelling concepts can be grouped as Monte Carlo, molecular dynamics, cellular automata models and today the promising phase field models. Regardless, it is still very difficult to find a comprehensive fundamental model to track the microstructure evolution along a given industrial process path. One reason is that important phenomena affecting solidification and microstructure occur in a wide range of length scales, from the atomic scale to the dimension of the macroscopic process. Today the range of the scales is too large to include all the phenomena in a single fundamental model. Another reason is that many systems never reach equilibrium, mainly due to the existence of metastable or long lived transient states, and these kinds of non-equilibrium states are still difficult to model accurately using fundamental concepts.

The models for estimating dendrite arm spacings or grain size in continuous casting are mainly based today on empirical data and statistical models. In the Laboratory of Metallurgy in Helsinki University of Technology, Finland, a solidification and microstructure model for steels, called IDS, has been developed since 1984. This model is based on a "grey box" methodology that combines both empirical and fundamental models. This is believed to be today the most realistic way to develop modelling tools for industrial processes. The term "grey box" means that some phenomena in the coupled tool are simulated by empirical and semi-empirical methods (black box) and some by fundamental principles (white box). Thus, IDS can be called as thermodynamic-kinetic-empirical tool.

In this present work dendrite arm spacings and grain size in continuous casting has been studied by mathematical

 © 2010 Wiley-VCH Verlag GmbH & Co. KGaA, Weinheim

modelling and experimental measurements. The calculations are compared with experimental results from steel plants. Two in-house tools have been used in the study, a heat transfer model called TEMPSIMU and the previously mentioned IDS. The effect of casting speed, superheat and secondary cooling on microstructure is also studied. The tools, calculation algorithms and the results are presented in this article.

Short Review of Equations for Dendrite Arm Spacings

Steel solidification in castings and ingots is dendritic. Fineness of dendritic structure is usually measured as dendrite arm spacing. A lot of different kind of empirical equations for estimation of secondary (λ_2) or primary (λ_1) arm spacing were published [1–8]. The equations are mainly based on experimental measurements and statistical modelling. Secondary arm spacing is determined as the mean value measured between secondary arms whose attachments to primary arms are clearly visible. In general, experimental measurements show good agreement with the time in which the arms are in contact with the liquid. This time is represented by the local solidification time (t_f), defined as the time spent between the liquidus and solidus temperatures. Instead of the local solidification time, it can also be used cooling rate (C_R), temperature gradient (G) or growth rate (R).

The equations of arm spacing are valid only for the conditions and composition range used in the study. It is generally found that the secondary arm spacing is related to the local solidification time or cooling rate by power laws as Eq. (2) shows. The primary arm spacing is usually described with G and R according to Equation (1). The typical equations used for λ_1 and λ_2 have the forms:

$$\lambda_1 = N \cdot G^{-l} \cdot R^{-m} \tag{1}$$

$$\lambda_2 = B \cdot C_R^{-n} = B(G \cdot R)^{-n} = M \cdot t_f^d \tag{2}$$

where N, l, m, B, n, M and d are parameters which depend mainly on the alloy composition. The solidification time is usually determined as:

$$t_f = \frac{T_L - T_S}{C_R} \tag{3}$$

where the T_L and T_S are the liquidus and solidus temperature, respectively. Many authors reported that λ_2 is related to the local solidification time [1–5]. It has been shown that λ_2 increases with time (t_f) spent in the mushy zone and increasing the cooling rate is also known to reduce λ_2. According to Suzuki et al. [6] the λ_2 is independent of the carbon content but influenced only by the average cooling rate. On the other hands, the variation of λ_2 with steel composition has been noted by other investigators [1–5, 8–10].

According to Won and Thomas [8] the λ_2 value decreases steeply with increasing carbon content from zero to its minimum value at 0.15% C and then increases with increasing carbon content until about 0.6% C. From 0.6 to 1.0% C, λ_2 decreases again with increasing carbon content. The results shown by Guo and Zhu [5] indicate that when the carbon content is below 0.15%, λ_2 decreases with an increase in the carbon content. If the carbon content is above this value, λ_2 remains constant. The author suggests that this phenomenon mainly occurs in the process of δ-ferrite solidification, owing to the peritectic reaction. Unlike the results showed by these authors, the empirical equation suggested by Cabrera-Marreno et al. [4] predicts an increasing λ_2-value with increasing carbon content. Cabrera-Marreno et al. [4] have also analysed the effects of processing variables on the arm spacing and have verified the influence of casting variables such as casting speed and tundish temperature on the dendrite arm spacing.

Most measurements of secondary arms have been performed on a small directionally solidified ingots equipped with thermocouples [1, 2, 6, 10]. The value of t_f can be read directly from the temperature/time recording. One problem is that the solidus temperature is difficult to determine accurately from the experiments because it is difficult to evaluate at which temperature the solidification is complete. In actual solidification process, it is also difficult to define the cooling rate, because it is not constant. So it is necessary to be careful when extrapolating experimental results to an industrial scale, since the solidification conditions are not the same.

As mentioned earlier, in the literature it is possible to find several expressions to predict arm spacings, many of them for a specific steel composition range [1, 7, 11, 12]. These equations lead to a large scatter of results in some cases when they are applied to real casting processes due to the absence of information about the valid composition ranges and calculation concepts of cooling rate, solidification time, etc. In the Helsinki University of Technology, equations for primary and secondary arm spacing have also been developed, taking into account the effect of composition and cooling conditions. These equations are applied to calculate the dendrite arm spacing inside a solidifying strand of industrial continuous casting machines. The results are compared with experimental measurements from the as-cast samples. The equations are coupled with the heat transfer (TEMPSIMU) and solidification model (IDS), which simulates the steels solidification in continuous casting and which is being developed also by the research group.

In-house Models Developed and used in this Study

TEMPSIMU - Heat Transfer Model for Continuous Casting. TEMPSIMU is a two-dimensional heat transfer model for the continuous casting of steel. In the case of steel continuous casting, the heat conduction in the casting direction is small and it can thus be ignored. Other assumptions made in the model are that (1) solidus and liquidus temperatures as well as all the other phase transformation temperatures are constant, (2) solidification takes place by directional growth, and (3) material behaviour is isotropic. TEMPSIMU calculates the strand temperatures and temperature related data such as the shell thickness in a

 © 2010 Wiley-VCH Verlag GmbH & Co. KGaA, Weinheim

two-dimensional cross-section of the strand on its passage through the caster. The heat transfer equation within the calculation domain is the following:

$$\rho \frac{\partial H}{\partial t} = \frac{\partial}{\partial x}\left(k \frac{\partial T}{\partial x}\right) + \frac{\partial}{\partial y}\left(k \frac{\partial T}{\partial y}\right) \quad (4)$$

The necessary material data are density (ρ), enthalpy (H), and thermal conductivity (k). Enthalpy also includes the phase change heats and the way in which the latent heats are released during the phase transformations. The convective heat transfer in the liquid pool due to the liquid flow is described with the effective thermal conductivity concept. The model equations are solved numerically using the finite element method in space and implicit finite difference method in time. The necessary input data for the simulation are strand dimensions, thermophysical material data, and machine and casting data. The model can be applied to casting of rectangular or centre square sections with or without rounded corners (slabs, blooms, billets) and to round sections. It can be used, for instance, to analyse the existing secondary cooling system and to study new alternatives (spray configurations, cooling water flow rates).

The mould heat flux is used as the boundary condition in the mould. The user gives the total amount of the heat flux and its distribution in the mould. Under the mould, the user can choose boundary conditions either for the zones (temperature, heat transfer coefficient or water flow rate) or for sprays and rolls (detailed option). Boundary conditions below the mould are defined numerically as:

$$k \frac{\partial T}{\partial n} + h(T - T_{ext1}) + \varepsilon\sigma(T^4 - T_{ext2}^4) = 0 \quad (5)$$

The terms describe the heat transfer by conduction, convection and radiation, respectively. Term h [$\mathrm{kW \cdot m^{-2}\,{}^{\circ}C^{-1}}$] is the heat transfer coefficient and T [$^{\circ}$C] is the strand temperature. In detailed option, depending on whether there is a roll or spraying area in question, T_{ext1} [$^{\circ}$C] is either the roll surface temperature or secondary cooling water temperature. Term ε is emissivity, term σ [$\mathrm{W \cdot m^{-2} \cdot {}^{\circ}C^{-4}}$] is Stefan-Boltzmann's constant and term T_{ext2} [$^{\circ}$C] is the temperature of air. In the secondary cooling zone the strand is held with rolls and between the rolls the nozzles spray the water or water-air mixture on the strand. When the strand passes between two rolls, four different cooling regions are accounted for in the model, as illustrated in **Figure 1**.

I. Roller contact area
II. Pre-nozzle area
III. Spraying area
IV. After spray and pool water area

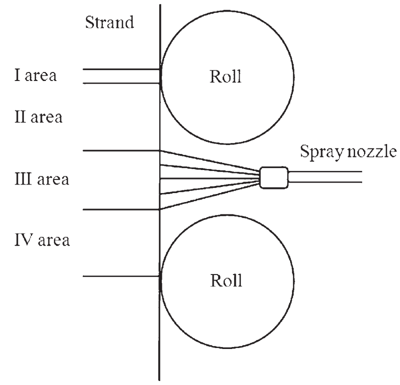

Figure 1. Cooling regions used in the model.

Material Data. To obtain reliable results from the heat transfer simulations, accurate thermophysical material data are needed. Usually these data are obtained from literature but very seldom all required data is found. The use of inaccurate material data can lead to considerable errors in calculations. Typical data needed are density, thermal conductivity, specific heat, phase transformation temperatures and the corresponding latent heat with the information how the latent heat is released during the phase transformations. The materials data used in the presented simulations were calculated using the IDS package presented in the following chapter. As the heat transfer model TEMPSIMU solves the model equations using fixed grids, the contraction of the steel is not calculated and taken into account. So, density cannot be varied either. In such a case, density should be that of the initial liquid and constant. By setting a constant value for density, the ingoing and the outgoing heat and mass flows in the model are the same. During solidification, however, the fluid is free to move in the interdendritic space and it more or less compensates the solidification contractions. To take this feeding into account, the density should be constant and that of the solidus temperature. Two calculations for a slab caster were made to test the effect of the density. The first calculation with the changing density gave 17.50 m for pool length and the second with the constant density 20.85 m. So, the difference in the pool length was over 3 meters. Thus, it is important to take care of the correct mass and heat balance.

IDS-Solidification and Microstructure Model. The IDS solidification analysis package is developed at the Helsinki University of Technology. The model is based on the thermodynamic theory connected to thermodynamic assessment data, as well as regression equations of experimental data. IDS includes two main modules, the IDS module and the ADC module. ADC is a semiempirical solid-state phase transformation model for steels and it simulates the austenite decomposition process below 1000 °C. Both modules have their own recommended composition ranges. The present version of the IDS module simulates the solidification of low-alloyed steels and stainless steels (Cr up to 24 wt% and Ni up to 16 wt%). The model applies a thermodynamic substitutional solution and magnetic ordering model and Fick's diffusion laws to determine the stable solution phases, liquid L, delta ferrite δ and austenite γ, and their fractions and compositions as a

 © 2010 Wiley-VCH Verlag GmbH & Co. KGaA, Weinheim

function of temperature. These calculations take into account the effect of solutes C, Si, Mn, P, S, Cr, Mo, Ni, Cu, Al, N, Nb, Ti, V, Ca, B, O, H, cooling rate and dendrite arm diameter. Assuming complete solute mixing in liquid the calculations can be made in one volume element set on the side of a dendrite arm. Also the formation of some binary compounds (MnS, NbC, NbN, TiC, TiN, VC, VN, AlN, BN, CO, SiO_2, Al_2O_3, CaO, CaS, Ti_3O_5, Ti_2O_3, TiO_2) can be simulated.

The ADC module, in the case of low-alloyed steels, the simulation involves the formation of proeutectoid ferrite, proeutectoid cementite, pearlite, bainite and martensite, and in the case of stainless steels, the formation of martensite only. The ADC model applies a thermodynamic substitutional solution and magnetic ordering model, a carbon diffusion model and special regression equations based on the German and the British CCT experiments. The simulation takes into account the effect of solutes C, Si, Mn, Cr, Mo, Ni, cooling rate and austenite grain size. The ADC model also calculates temperatures Ae_3 and A_{cm} taking into account the effect of the 18 solutes elements of IDS simulation mentioned above. The IDS package also calculates solidification-related thermophysical properties (e.g. enthalpy, specific heat, density and thermal conductivity) from the liquid state down to the room temperature. The calculations of the IDS package have been compared with many experimental measurements.

IDS also calculates some microstructural features as austenite grain size and secondary dendrite arm spacing. For low alloyed steels, IDS estimates the as-cast austenite grain size, d_G [μm] according to

$$d_G = 1841 - 1836 \cdot \frac{\exp(C_R)}{1+\exp(C_R)} + 3.44 \cdot 10^{-5} \cdot \exp\left(\frac{T^{\gamma}}{80}\right) \tag{6}$$

Here, C_R [$^{\circ}\mathrm{C}\cdot\mathrm{s}^{-1}$] refers to the nodal cooling rates below the liquidus temperature, which can be obtained with the heat transfer model and T^{γ} [°C] is a maximum temperature of a totally austenitic structure obtained with the IDS model. This equation was optimised using the measured grain size data of Yasumoto et al. [13] and it shows that with lower cooling rate and higher value of T^{γ}, the grain size is coarser. This trend is logical since a low cooling rate leaves more time for austenite grains to grow and a high temperature is related to a higher growth rate. The exponential form was chosen for the cooling rate to prevent unrealistic predictions of d_G beyond the studied cooling rate region of 0.5 to 1.5 $^{\circ}\mathrm{C}\cdot\mathrm{s}^{-1}$.

The present study introduces new regression equations for the calculation of primary and secondary dendrite arm spacing in multicomponent steels, taking into account the effect of cooling rate and composition. Both equations were optimised using the experimental measurements of the literature. The primary arm spacing is usually described by the equation type (1) but here the equation is presented as a function of cooling rate. The new λ_1 and λ_2 [μm] equations are expressed by:

$$\begin{aligned}\lambda_1 = {} & 400(C_R)^{-0.35} \\ & \cdot \exp(-(0.5647\%C + 0.2143\%Si \\ & + 0.0110\%Mn + 0.0999\%Cr + 0.3765\%Mo \\ & + 0.0282\%Ni - 0.35115\%C^2 \\ & - 0.00345\%Cr^2 - 0.00043\%Ni^2 \\ & - 0.01052\%Cr\%C + 0.00144\%Cr\%Ni)^{0.4})\end{aligned} \tag{7}$$

$$\begin{aligned}\lambda_2 = {} & 200(C_R)^{-0.33} \\ & \times \exp(-(0.6844\%C + 0.0069\%Si \\ & + 0.0674\%Mn + 0.1412\%Cr + 0.0057\%Mo \\ & + 0.1259\%Ni - 0.14788\%C^2 \\ & - 0.00387\%Cr^2 - 0.00101\%Ni^2 \\ & + 0.10295\%Cr\%C - 0.00456\%Cr\%Ni)^{0.4})\end{aligned} \tag{8}$$

where C_R [$^{\circ}\mathrm{C}\cdot\mathrm{s}^{-1}$] is the cooling rate in the mushy zone obtained with the heat transfer model and the composition is given in wt%. The Eq. (7) and Eq. (8) were optimized using the experimental data of sources [1, 6, 10, 14–21]. Careful selection of data was carried out to exclude such experimental data from the analysis which did not correlate well with either the calculations or the other experimental data. The reason for the use of the cooling rate in the equations above is that it can easily be related to any casting process but parameters R and G cannot, as they can have numerous combinations. The validation of Eq. (7) and Eq. (8) is presented in **Figure 2** and **Figure 3**, respectively. The new equation for λ_2 gives better correlation between the calculated and experimental λ_2 than two separated equations presented in the earlier study [22].

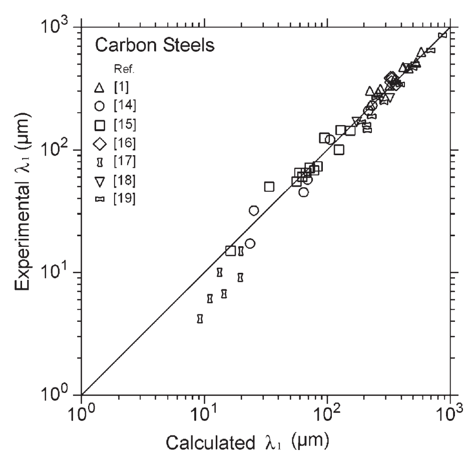

Figure 2. Calculated vs. experimental λ_1.

 © 2010 Wiley-VCH Verlag GmbH & Co. KGaA, Weinheim

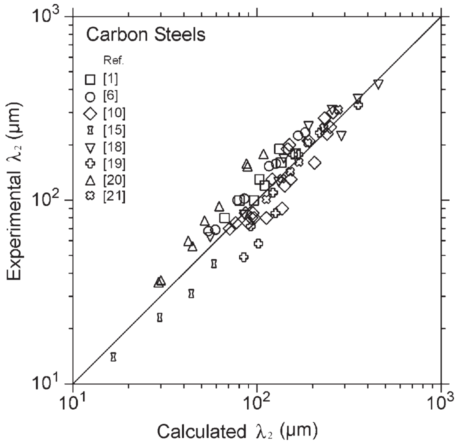

Figure 3. Calculated vs. experimental λ_2.

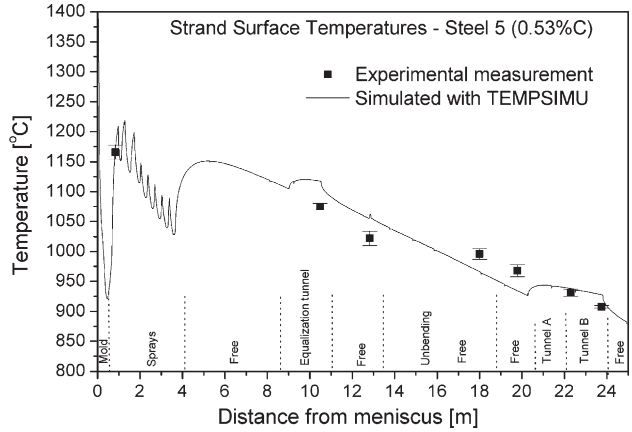

Figure 4. Temperatures of the strand surface during casting of steel 05 - 150 parabolic mold.

Coupling of the TEMPSIMU and IDS Models. The IDS and TEMPSIMU models have been coupled to predict the microstructure evolution in continuous casting. IDS calculates the thermophysical material data for TEMPSIMU, which then calculates the cooling rates at each nodal point in the strand. IDS then again calculates the microstructure evolutions using these cooling rates. The procedure is as follows:

1. Assume a cooling rate for the solidification and for the austenite decomposition (ADC cooling rate).
2. IDS: calculate the material properties for the steel using the assumed cooling rates.
3. TEMPSIMU: Calculate the temperatures and the actual cooling rates through the strand.
4. If the calculated actual cooling rates on average match the assumed cooling rates, go to step (5). Otherwise, go back to step (1).
5. IDS: Calculate the microstructural evolutions through the strand using the local cooling rates and the local steel composition. Normally, the austenite decomposition model applies the nominal or the interdendritic composition of the steel in the calculations. However, the macrosegregation profiles of solutes, if known, can also be used as the input data.

Validation of the TEMPSIMU Heat Transfer Model. The steady state heat transfer model, TEMPSIMU was validated by measuring shell thicknesses and surface temperatures in different locations of the strand. Measurements were performed with a curved type slab caster at Ruukki Steel in Finland. Shell thickness was determined by using a wedge technique and temperatures were measured with pyrometers. In the wedge technique, a wedge is fed between two rolls of a caster. As the strand moves on, the wedge moves between the roll and the strand. The wedge causes tensile stress resulting in cracks in the solidification front of the strand. Shell thickness is then determined from the crack tip locations in the strand specimens. The simulations with TEMPSIMU showed good agreement with the shell thickness and temperature measurements [22].

The TEMPSIMU model was also validated by surface temperature measurements in a Brazilian steel plant. The experimental strand surface temperatures were obtained using non-contact infrared optical mobile pyrometers located at selected positions along the foot-roll, secondary cooling zones and the radiation zones [23]. The data were analysed and their average values were determined in a function of time. **Figure 4** shows strand temperatures measured by pyrometers in different positions along the machine during casting for the carbon Steel 5 (see Table 1) as well as the simulation with TEMPSIMU. The results showed good agreement when experimental and simulated results were compared.

Experimental - Case Studies

In order to investigate the effect of steel grade and casting parameters on dendrite arm spacing and grain size, five types of steels were selected for this study. The steels were cast in a Brazilian billet caster with section size 150 mm × 150 mm. The steel composition, tundish temperature and casting speeds are presented in **Table 1**. The liquidus and solidus temperatures in the Table 1 are determined using the IDS package. For the metallographic study many samples from the as-cast billets were taken. After surface adequacy, the samples were ground, polished and finally etched with 10% Nital reagent. In order to reveal the dendritic structure, small samples were cut, polished and etched with solution of 40 g $FeCl_3$, 3 g $CuCl_2$, 4 ml HCl, 500 ml water.

Secondary dendrite arm spacing was measured by averaging the distance between adjacent side branches on the longitudinal section of a primary arm. Measures of λ_2 were made on billets samples in regions from surface to the centre of the billet cross section. The samples were divided into 10 parts as shown in **Figure 5**. For each part around 20 measurements were made to obtain the average values as well as the maximum, minimum and standard deviation of the λ_2. This method is based on measuring the λ_2 by counting

 © 2010 Wiley-VCH Verlag GmbH & Co. KGaA, Weinheim

Table 1. Chemical compositions and process parameters of the steels.

Steels	Composition (wt.%)									IDS		Process parameters	
	C	Cr	Mn	Mo	Ni	Si	S	Al	Nb	T_L [°C]	Ts [°C]	Pouring Temperature [°C]	Casting Speed [m min^{-1}]
1	0.07	0.06	1.02	0.024	0.09	0.01	0.032	0.002	0.003	1526	1479	1576	1.7
2	0.16	1.04	1.12	0.04	0.17	0.23	0.024	0.02	0.016	1514	1462	1540	2.3
3	0.21	0.47	0.77	0.16	0.45	0.23	0.028	0.027	0.001	1511	1452	1542	2.2
4	0.45	0.11	0.80	0.022	0.10	0.27	0.021	0.014	0.002	1493	1413	1515	2.2
5	0.53	0.66	0.67	0.04	0.11	1.30	0.007	0.012	0.016	1471	1358	1514	2.0

the number of arms over a certain length of a primary dendrite arm axis. The images were acquired on an optical microscope using a CCD camera over each selected position. The calibration of the images and subsequent measurement of the λ_2 were made with image analyser software. It is important to mention that in the region next to the surface the samples have presented structure with high refinement and thus it was not possible to carry through measurements of λ_2.

Figure 6 shows the macrograph and micrograph of Steel 3. The macrostructure characterised by columnar and equiaxial grains (Figure 6a) and the dendritic microstructure (Figure 6b) showing the columnar to equiaxed transition (CET) can be observed.

Figure 7a-e shows the experimental results of the secondary dendrite spacing for the steels studied from the surface to the centre including the average columnar to equiaxed transition (CET). All these castings were simulated using TEMPSIMU and IDS tools. Figure 7 also shows the cooling rate calculated with TEMPSIMU. The experimental λ_2 were compared with the calculated λ_2 using the Eq. (8). The calculated results are in reasonably agreement with the measured values, except for the case No. 1 (Steel 1). For this steel the spacing seems to be clearly higher than for the other ones. Won and Thomas [8] and Guo and Zhu [5] found that the arm spacing decreases with the carbon content up to 0.15% and after this increases slightly (Won and Thomas [8]: up to C = 0.6%) or remains constant. This effect with low carbon content is believed to be related to the δ-ferrite solidification. It seems that our equation underestimates slightly the very low carbon steel grades. The results also indicate that λ_2 increases with a decrease in cooling rate, as expected.

One very important question is how to calculate the cooling rate for the equations. In continuous casting the cooling rate during solidification is not constant but varying. For the presented cases (Fig 7 a-e) the cooling rate was calculated and assumed to be the average rate between the liquidus temperature (T_l) and the liquidus minus five degrees (T_l -5 °C). **Figure 8** shows the λ_2 values when the cooling rate is calculated from the temperature range T_l -5 °C, T_l -10 °C and T_l -T_s. The results are very different. The results indicate that a wrong definition of the measurement range can lead to errors. The exact way is not clear in the literature. According to our results, the cooling rate should be calculated from the conditions close to the dendrite tip, i.e. from the conditions between T_l and T_l -5 °C.

Figure 9 presents the experimental results of λ_1 and λ_2 values from surface to centre of the strand for different steel types of the Table 1. The results show that the spacing depends on the carbon contents and is highest for the low carbon steels as mentioned already before. It is also the highest temperature of a totally austenitic structure without δ-ferrite formation and peritectic reaction seem to effect the dendrite growth phenomena.

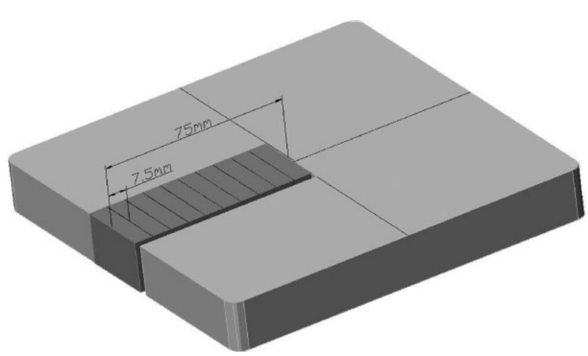

Figure 5. Analysing points on the transversal billet sample.

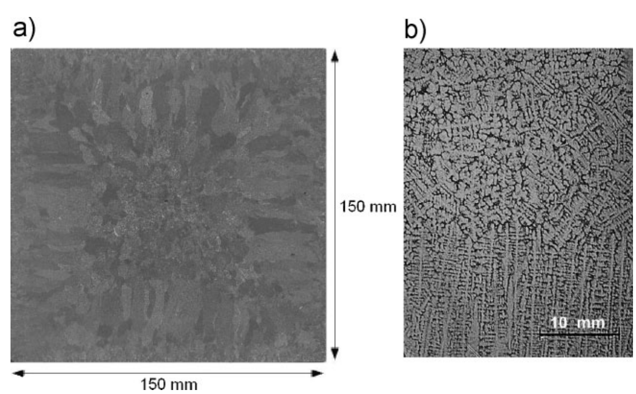

Figure 6. For Steel 3: a) Macrograph of the cross section of the billet; b) Micrograph of the areas between 20 mm (columnar) and 60 mm (equiaxed) from the surface.

 © 2010 Wiley-VCH Verlag GmbH & Co. KGaA, Weinheim

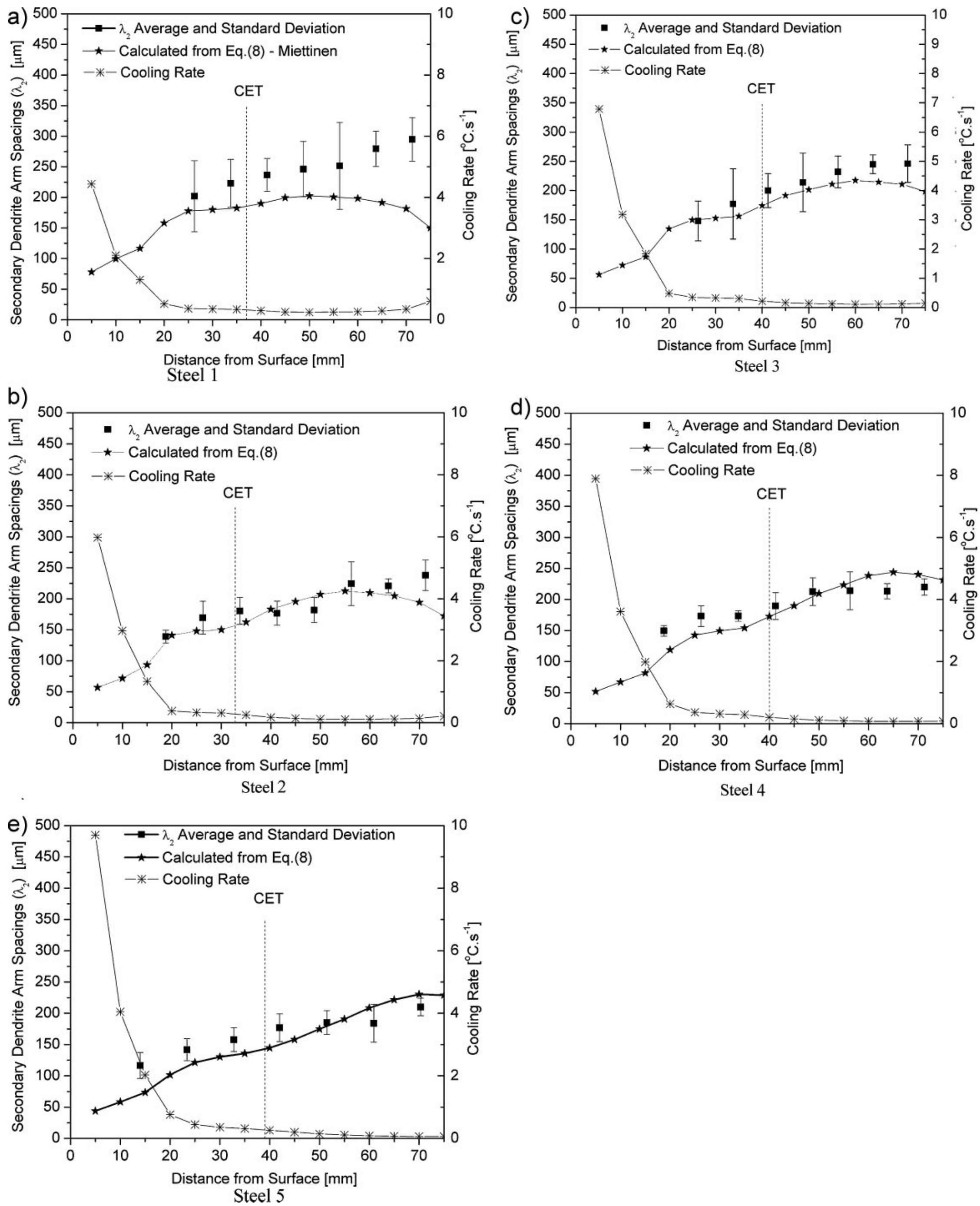

Figure 7. Experimental and calculated secondary dendrite arm spacing (λ_2) for the cases in Table 1.

Relationship between λ_1 and λ_2

The λ_1/λ_2 ratio is an important parameter to estimate the permeability of the interdendritic channels in the mushy zone that depends on the liquid fraction and the primary and secondary dendrite arm spacing; and hence to avoid interdendritic microporosity formation during solidification [24]. Cicutti and Boeri [7] have calculated the λ_1/λ_2 relation for a slab continuous casting. For steel with 0.15%C, the model predicted a λ_1/λ_2 ratio of 2.6, which was almost constant along the slab thickness. Guo and Zhu [5] have analysed the relationship between λ_1/λ_2 and carbon content at different cooling rates. The results indicated that λ_1/λ_2 ratio increases with higher cooling rates and remains almost constant when analysed at a constant cooling rate, with only a small increase in the λ_1/λ_2 values for steels around 0.15%C. The variation of the λ_1/λ_2 was found to be around 1.6–4.2 for slab casting steels below 0.4% C. **Figure 10a**

 © 2010 Wiley-VCH Verlag GmbH & Co. KGaA, Weinheim

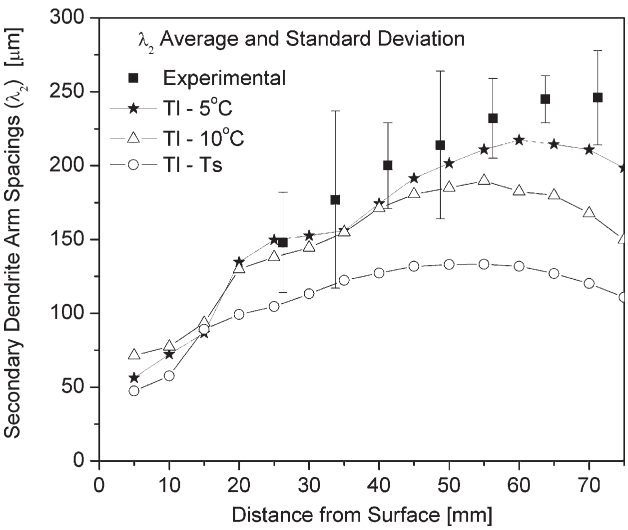

Figure 8. λ_2 values calculated using cooling rates calculated from different temperature ranges.

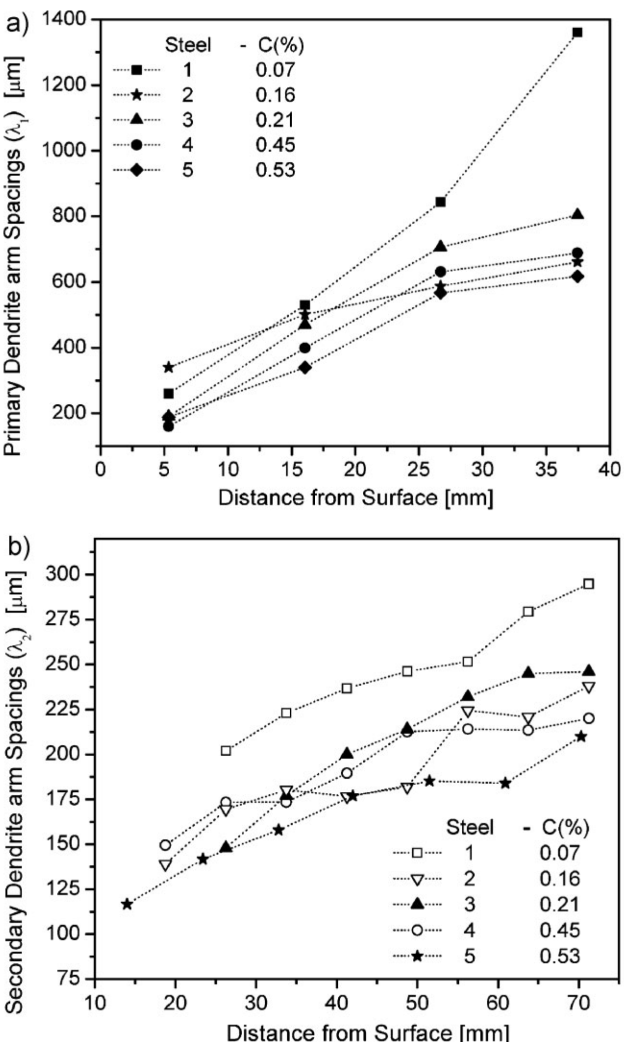

Figure 9. Comparison between the measured primary (a) and secondary (b) dendrite arm spacing of the steels presented Table 1.

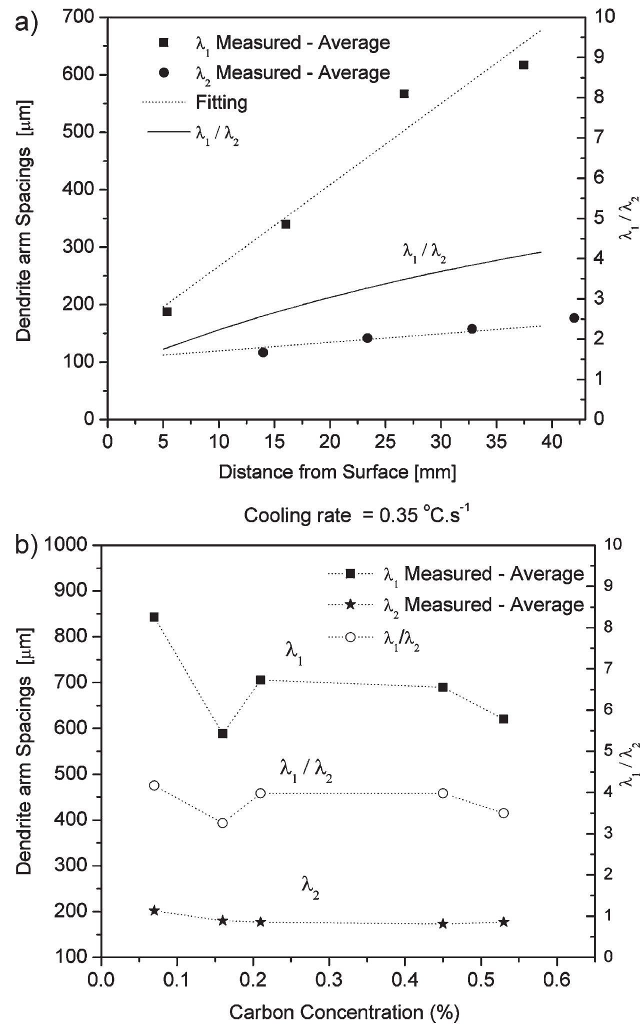

Figure 10. (a) Relationship between λ_1/λ_2 for the steel 5. (b) Comparison between average λ_1 and λ_2 for the studied steels with constant cooling rate.

shows the variation of the λ_1/λ_2 ratio across the billet thickness. The values were calculated from fitting curves of the experimental data. Results indicate that λ_1/λ_2 increases as a function from the surface and this differs from the results of Cicutti and Boeri [7] and Guo and Zhu [5]. For constant cooling rate but different carbon content, the relation is almost constant with only a small decrease for steels about 0.16% C (**Figure 10b**). This phenomenon is also different than presented by Guo and Zhu [5], because they found a small increase around 0.15% C. In this study, the ratio was found to be in the range 1.2 to 4.7 as presented in the Figure 10a.

Figure 11 shows the calculated and measured data for the austenite grain size. These experiments were carried out in a bloom caster of Imatra Steel, Finland, and the steel composition is given in **Table 2**. The casting was simulated by TEMPSIMU and IDS and the grain size calculated according to the Equation (6). The finer grains near the surface area are due to the high cooling rates below the

 © 2010 Wiley-VCH Verlag GmbH & Co. KGaA, Weinheim

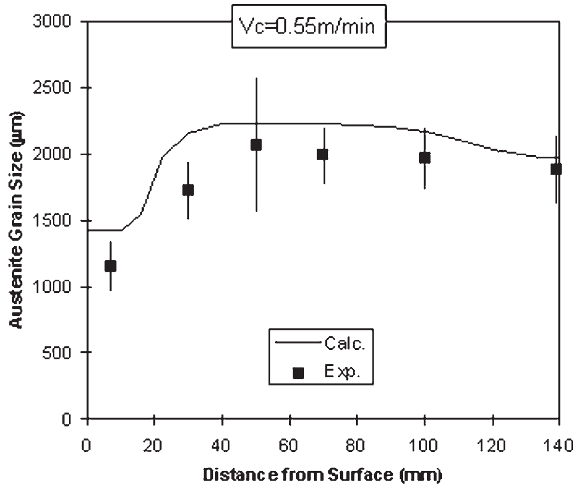

Figure 11. Calculated austenite grain size distribution with some experimentally measured data points in as-cast bloom (IDS + TEMPSIMU –simulations) [22].

solidus in this area. The calculated distributions correlate well with the measured data taking into account that the grain size is not so accurate term to measure.

It is known that the austenite grain size depends on carbon content and on cooling rate. This was earlier studied using the IDS tool [22]. The calculation results are presented in **Figure 12**. It can be seen that the grain size is the bigger the higher is the T^{γ} temperature and the slower is the cooling rate below the solidification. The biggest grain size was obtained for the carbon content of about 0.15%. Equation (6) is used in these calculations.

Influence of Casting Parameters on Dendrite Arm Spacing and Grain Size

In the current subject the effect of casting speed, superheat in tundish and the effect of secondary cooling on arm spacing and grain size were investigated using the developed tools and equations. Steel 3 was used in this study. The effect of casting speed is presented in **Figure 13**. The casting speeds were 1.5 and 2.5 $m \cdot min^{-1}$. The effect is not so big. The cooling rate is slightly higher with lower casting speed resulting in smaller arm spacing and finer grain size. Larger dendrite spacing is observed with an increase of the casting speed. This is due to the lower residence time of the strand in the mould zone and in the secondary cooling zone; similar results were obtained by Cabrera-Marrero et al. [4]. The effect of secondary cooling or superheat on the arm spacing or grain size is very small. It means that arm spacing and grain size can hardly be influenced by these process parameters (**Figure 14 and 15**).

Table 2. Steel composition of the Finnish study, in wt.%.

C	Si	Mn	P	S	Cr	Ni	Mo	Ti	Cu	Al
0.41	0.248	0.904	0.009	0.025	1.022	0.198	0.244	0.005	0.182	0.056

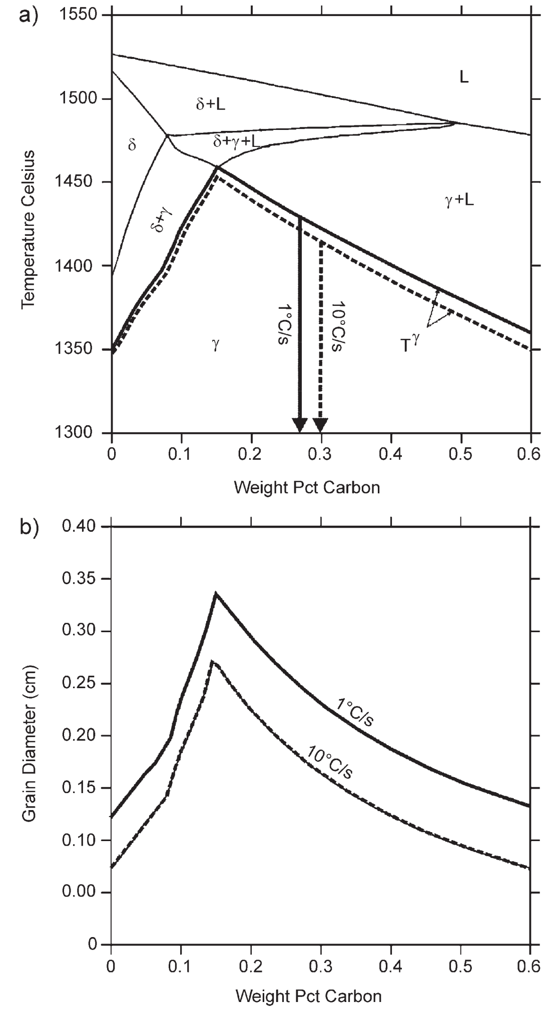

Figure 12. Simulated example: the effect of carbon content and cooling rate on the T^{γ} temperature (a) and austenite grain size (b) in steel 0-0.6%C + 0.3%Si + 1%Mn + 0.02%P + 0.02%S [22].

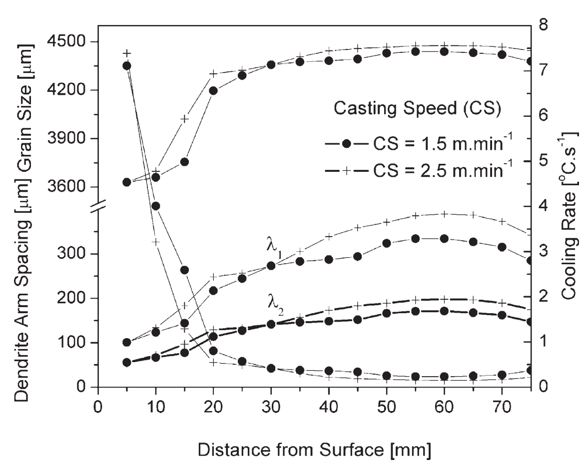

Figure 13. Comparison of λ_1, λ_2 and grain size simulated at different casting speed for the Steel 3.

 © 2010 Wiley-VCH Verlag GmbH & Co. KGaA, Weinheim

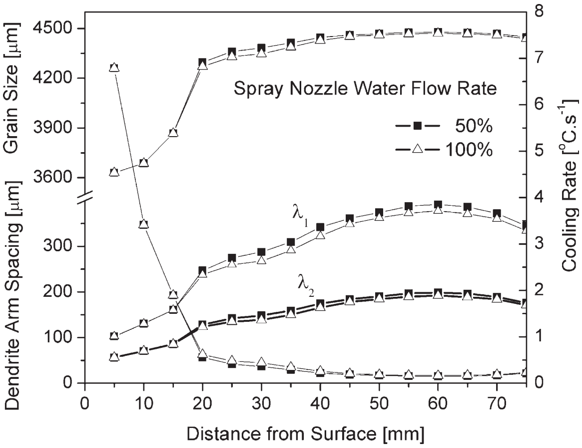

Figure 14. Comparison of λ_1, λ_2 and grain size simulated at different water flow in the secondary cooling for the Steel 3.

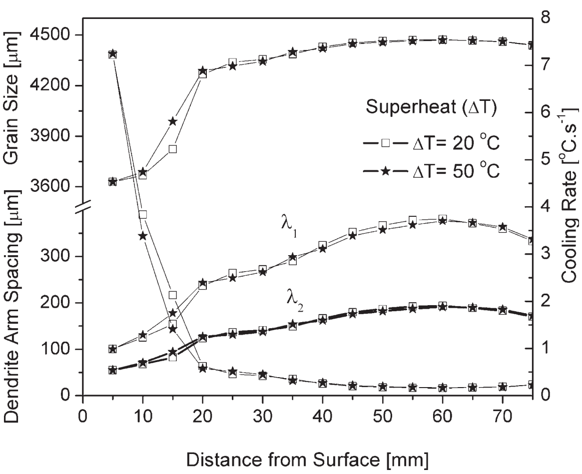

Figure 15. Comparison of λ_1, λ_2 and grain size simulated at different superheat for the Steel 3.

Conclusions

Expressions for the primary and secondary dendrite arm spacing as a function of cooling rate and steel composition are proposed. An expression for the calculation of austenite grain diameter is also presented.

The models are validated by comparing the calculated results with experimental ones from steel plants. It seems that the models quite accurately predict the micro-structural features like dendrite arm spacing and as-cast austenite grain size.

The influence of casting parameters is also studied. Although the dendrite arm spacing and grain size are strongly influenced by cooling rate and steel composition, the microstructure did not change very much when casting parameters like casting speed, tundish temperature and secondary cooling intensity were changed.

In **Figure 16** experimental values for secondary dendrite arm spacing for different steels obtained from the literature are presented as a function of carbon content, in the cooling rate range of 0.3 to 0.5 $^\circ C \cdot s^{-1}$. It can be seen that the spacing increases a lot with the low carbon steels compared to higher carbon steels. This means that it would be good to make two separate models for low carbon and high carbon steels. In this paper only a single formula is used and presented but in the future, two formulas will be determined and even better results are expected.

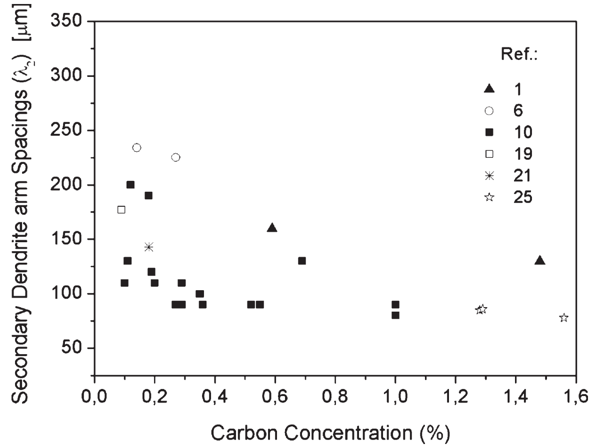

Figure 16. Experimental λ_2 values for different steels as a function of carbon content in the cooling rate range from 0.3 to 0.5 $^\circ C \cdot s^{-1}$.

Acknowledgements

The authors would like to thank many people in industry and universities for cooperation, support and help. We would also like to thank agency National Council for Scientific and Technological Development of Brazil (CNPq) as well as Finnish steel industry and Finnish Technology Development Centre (TEKES) for the financial support.

References

[1] H. Jacobi, K. Schwerdtfeger: Metallurgical and Materials Transactions A, 7A (1976), No. 5, 811–820.
[2] R. Pierer, C. Bernhard: J Mater Sci, 43 (2008), 6938–6943.
[3] M. El-Bealy M., B. G. Thomas: Metallurgical and Materials Transactions B, 27B (1996), No. 4, 689–693.
[4] J. M. Cabrera-Marrero, V. Carreno-Galindo, R. D. Morales, F. Chavez-Alcala: ISIJ International, 38 (1998), No. 8, 812–821.
[5] W. Guo, M.-Y. Zhu: Journal of Iron and Steel Research International, 16 (2009), No. 1, 17–21.
[6] A. Suzuki, T. Suzuki, Y. Nagaoka, Y. Iwata: Nippon Kinzoku Gakkaishi, 32 (1968), 1301–1305.
[7] C. Cicutti, R. Boeri: Scripta Materialia, 45 (2001), No. 12, 1455–1460.
[8] Y. M. Won, B. G. Thomas: Metallurgical and Materials Transactions A, 32A (2001), 1755–1767.
[9] J. Miettinen, H. Kytönen: Calculation of Dendrite Arm Spacing in solidified Steels. Report TKK-MT-186, Helsinki University of Technology Publications in Materials Science and Engineering, TKK, Espoo, 2006, pp. 1–20.
[10] Guide to the Solidification of Steels, ed. By Jernkontoret, Stockholm, 1977, pp. 1–150.
[11] J. E. Spinelli, J. P. Tosetti, C. A. Santos, J. A. Spim, A. Garcia: Journal of Materials Processing Technology, 150 (2004), 255–262.

 © 2010 Wiley-VCH Verlag GmbH & Co. KGaA, Weinheim

[12] M. Wolf, W. Clyne, W. Kurz: Archiv Eisenhüttenwesen, 53 (1982), 91–96.
[13] K. Yasumoto, T. Nagamichi, Y. Maehara, K. Gunji: Tetsu-to-Hagané, 73 (1987), 1738.
[14] T. Edvardsson, H. Fredriksson, I. Svensson: Metall. Sci. 10 (1976), 298–306.
[15] M. Wolf: Doctoral Thesis, ETH Lausanne, 1978.
[16] M. Suzuki, T. Kitagawa, S. Miyahara: Tetsu-to-Hagane, 71 (1985), 1034.
[17] J. E. Gould: Welding Research Supplement, 73 (1994), 91–100.
[18] M. Imagumbai: ISIJ International, 134 (1994), 574–583 and 896–905.
[19] H. Jacobi, K. Wünnenberg: Steel Research, 70 (1999), 362–367.
[20] K. Schwerdtfeger: Archiv Eisenhüttenwesen, 41 (1970), 923–937.
[21] B. Weisberger, M. Hecht, K. Harste: Steel Research, 70 (1999), 403–411.
[22] S. Louhenkilpi, J. Miettinen, L. Holappa: ISIJ International, 46 (2006), No. 6, 914–920.
[23] C. A. Santos, E. L. Fortaleza, C. R. F. Ferreira, J. A. Spim, A. Garcia: Modelling Simul. Mater. Sci. Eng., 13 (2005), 1071–1087.
[24] R. G. Santos, M. L. N. M. Melo: Materials Science and Engineering A, 391 (2005), 151–158.
[25] T. Okamoto, S. Matsuo, K. Kishitake: Tetsu-to-Hagane, 63 (1977), 936–942.

© 2010 Wiley-VCH Verlag GmbH & Co. KGaA, Weinheim